PROCEEDINGS

OF THE

THIRD JOINT SYMPOSIUM

ON THE

NATURAL HISTORY AND GEOLOGY OF THE BAHAMAS

Edited by
David Griffing, Mark Kuhlmann and Troy Dexter

ORGANIZER:

Troy A. Dexter

Executive Director
Gerace Research Centre
University of The Bahamas
San Salvador, The Bahamas

2023

NEW ADVANCES IN LONG-TERM MONITORING OF STORM-DEPOSITED BOULDER RIDGES ALONG ROCKY SHORELINES OF SAN SALVADOR ISLAND, BAHAMAS

Bosiljka Glumac*, Ursula Miguel, and H. Allen Curran

*Corresponding author; e-mail: bglumac@smith.edu; phone: 413-531-6801

Department of Geosciences, Smith College, Northampton, MA 01063 USA

ABSTRACT

Beginning in January 2012, we have monitored two boulder ridges on San Salvador: Singer Bar Point (SBP, length ~790 m) along the reef- and lagoon-protected northern coast and The Gulf (TG, length ~460 m) on the island's high-energy southern coast. This long-term monitoring aims at documenting changes in ridge morphology and distribution, and the direction and amount of movement of individual boulders to gain insights into the intensity and effects of storms on these coastal areas.

In the initial stage of our investigations, the largest boulders from each site were photographed, GPS-located, measured, and characterized by composition and morphology. Boulders at SBP are generally smaller (15 total; ~150-4000 kg; with most <1500 kg) than those at TG (12 original; ~700-6500 kg; most >1000 kg). Our monitoring surveys from January 2013, 2016, and 2017, after Hurricanes Sandy (October 2012), Joaquin (October 2015), and Matthew (October 2016), respectively, indicated only modest modifications at SBP, and major changes to TG, where we were unable to relocate 2 boulders post-Sandy, and 5 of the 10 remaining original boulders after Joaquin. Two TG boulders, weighing ~1 and 3 tons, were transported inland to the NNW by 20 and 26 meters, respectively during Hurricane Joaquin, and there was significant movement inland of the entire boulder ridge.

Even though documentation of boulder movement allows calculation of minimum flow velocity needed to initiate transport, our experience indicated that lack of adequate tagging made it challenging or impossible to relocate individual boulders after major storms. This problem was addressed by the application of RFID (radio frequency identification) tagging in June 2019. With a larger cohort of boulders now tagged, our monitoring program is well established to continue into the future, as passive tags are inductively charged by the reader and can remain operational for decades. Drilling to insert small tags (23 and 32 mm long, and <4 mm in diameter) is minimally destructive and also allows tagging of pebbles and cobbles. This is especially important for monitoring at SBP where large boulders are not moved often or much by waves, but smaller-sized sediment movement is significant during storms.

INTRODUCTION TO STUDY AREA AND METHODS

Coastal ridges made primarily of limestone boulders (clasts >25 cm in diameter) are common but little studied features along rocky shorelines on many islands of the Bahama Archipelago. Origin and transport of large individual boulders in the Bahamas, especially the scattered "megaboulders" on North Eleuthera, however, has been hotly debated during the past two decades (Hearty 1997; Panuska *et al.* 2002; Kelletat *et al.* 2004; Mylroie 2008, 2018; Kindler *et al.* 2010; Hearty and Tormey 2017; Rovere *et*

al. 2017, 2018). Even though the debate over transport mechanisms for these large boulders is ongoing, the results of recent studies from the northern Atlantic of western Ireland unequivocally proved that storm waves can move limestone megaboulders on cliffs located 10 meters or higher above high-water level (Cox *et al.* 2012, 2018). Similarly, observations from San Salvador Island in the aftermath of 1999 Hurricane Floyd (Curran *et al.* 2001; Walker *et al.* 2001) and 2004 Hurricane Frances (Niemi *et al.* 2008; Niemi 2017) documented formation and transport of rock boulders by high energy storm waves.

Our long-term monitoring of the impact of storms on the rocky coastline of San Salvador since January 2012 has focused on two prominent boulder ridges, one along the reef- and lagoon-protected northern coast west of and around Singer Bar Point (SBP), and the other on the high-energy southern coast of the island west of The Gulf (TG; Figure 1). Singer Bar point is located about 1 km (0.6 miles) west of the Gerace Research Centre (GRC) campus. The total length of this boulder ridge is ~790 m, and this study focused on an area ~450 m long, located to the east of the boat ramp, which is about 1.5 km (0.9 miles) west along the Queen's Highway from GRC (Figure 1B). Similarly, even though the boulder ridge at TG is ~460 m, we focused primarily on the ~200 m section located on the coastal cliff between The Cut and The Gulf embayments (Figure 1B).

Both boulder ridges were deposited by storm waves, and comparison of these two coastlines of very different energy-level characteristics provides insight into the relationship between wave intensity and boulder formation, morphology, and transport. The main objectives of this study are to gather information about the distribution and morphology of these boulder ridges, and on the movement of individual boulders to better understand the influence of storms on geomorphology of the coastal landscape. The results of such long-term monitoring efforts should be informative to decision making regarding future coastal development on this and similar coastal areas on

other Bahamian islands. Cumulative data also will provide information for continuing documentation of boulder transport by storm waves, and development of criteria for analyzing coastal boulder deposits in general (e.g., Cox *et al.* 2018).
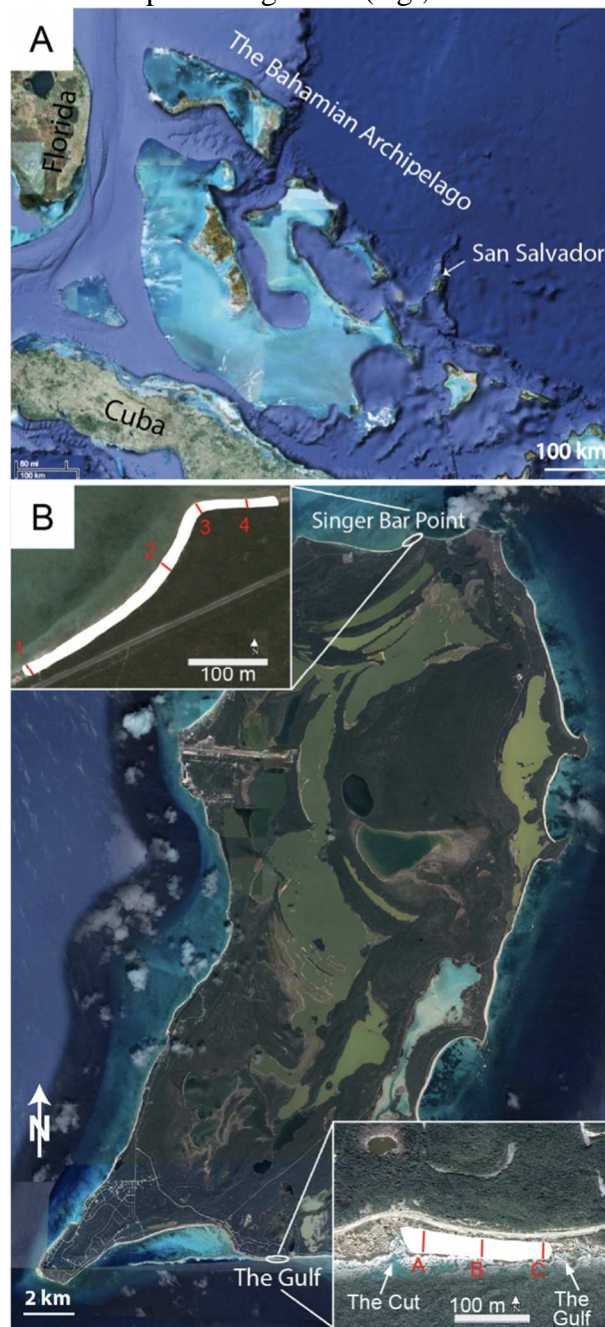

Figure 1. Study area. A) The Bahama Archipelago, with Florida and Cuba for context, and San Salvador Island. B) Map of San Salvador with the two study sites labeled: Singer Bar Point (SBP) along the relatively low-energy north coast, and The Gulf (TG) on the high-energy south coast. Insets show the study sites outlined in white, with red lines and labels marking the location of profiles shown in Figure 2 (source: Google Earth).

Initial fieldwork for this study was conducted on San Salvador in January 2012 after Hurricane Irene passed as a Category 2 storm about 80 km (50 miles) to the SW of the island in August 2011 (National Hurricane Center). This initial work included GPS data-point recording and measurements of coast-normal transects (4 for SBP and 3 for TG) over the boulder ridges (Figure 1B). The largest boulders from each site (15 SBP and 12 TG boulders) were photographed and located with GPS coordinates for future reference. Boulders were measured (length, width, thickness), characterized by composition (subtidal calcarenite, coral rubblestone, eolianite, paleosol), shape (tabular or irregular), and degree of roundness. Approximate boulder weight was determined using average limestone density of 2.4 g/cm^3 and by subtracting 20% from calculated values to account for irregular boulder size and porosity distribution.

Additional field observations were made in early 2013 to assess the impact of October 2012 Hurricane Sandy, in January 2016 to document modifications by Hurricane Joaquin that passed directly over San Salvador in October 2015, and in January 2017 after October 2016 Hurricane Matthew. While Hurricane Matthew passed too far west of San Salvador to have any major impact on the island, this research documented significant modifications by Hurricane Sandy and especially by Joaquin, which are detailed here. Documentation of boulder movement also allowed calculation of minimum flow velocity required to initiate their transport using equations from Nandasena *et al.* (2011), which are dependent on boulder size, density of boulders and water, coefficients of lift, drag, gravity, and slope angle.

In January 2016, we also initiated use of drone technology for high-resolution imaging of the study areas (Perlmutter *et al.* 2016). Subsequent drone imaging was conducted in January 2017 and 2020, and in June 2019 we also implemented RFID (radio frequency identification) technology to tag boulders at each study site to aid in their relocation after major storm events. This proved necessary because we learned from experience that when boulders move, even very large ones, they can be difficult to relocate.

RFID technology uses small (23 and 32 mm long and <4 mm in diameter) PIT (passive integrated transponder) tags. These passive tags have unique identifying numbers that are recorded by an RFID reader at a short distance, depending on tag size and antenna design. The tags are inductively charged by the reader, and because they do not have a battery, they can theoretically remain operational indefinitely. Their small size and relatively low cost allows tagging of a large number of clasts, which in addition to boulders can also include smaller cobbles and pebbles. Moreover, tagging of particles is minimally invasive. Small holes (only about 5 mm in diameter and up to 40 mm deep) are drilled into boulder surfaces using a hand-held, battery-operated hammer drill with a carbide drill bit. Holes are lined with silicone adhesive and then patched with water-resistant epoxy putty whose color closely matches that of the rock surface.

These advances in our long-term monitoring of storm-deposited boulder ridges significantly increased our database and are expected to add significantly to our efforts to communicate information about vulnerability to hurricanes with stakeholders on San Salvador and elsewhere in The Bahamas. Such efforts are becoming increasingly important as the consequences of changing climate and rising sea levels are amplified by powerful storms, exemplified by the devastating impact of Hurricane Dorian on Grand Bahama and Abaco Islands in September 2019.

RESULTS

Initial Survey (January 2012)
Our initial work in January 2012 described the Singer Bar Point (SBP) boulder ridge on the low energy north coast as wide (up to 14 m) and with a low crest (~1.5 m above mean sea level), whereas The Gulf (TG) ridge on the high energy south coast was generally narrower, with a sharp crest located on a cliff-bench 3-5 m above mean sea level (Figure 2; Table 1). Profiles through the boulder ridges were constructed from the measured transects (Figures 1B and 2), the largest

boulders along the transects were documented (Table 2), and 15 additional large boulders from SBP and 12 from TG were photographed and located with GPS coordinates (Table 3).

The largest boulders at SBP are generally smaller (~150-4000 kg; with most <1500 kg) and more rounded than those at TG (~700-4500 kg; with all but one >1000 kg; Tables 1-3).
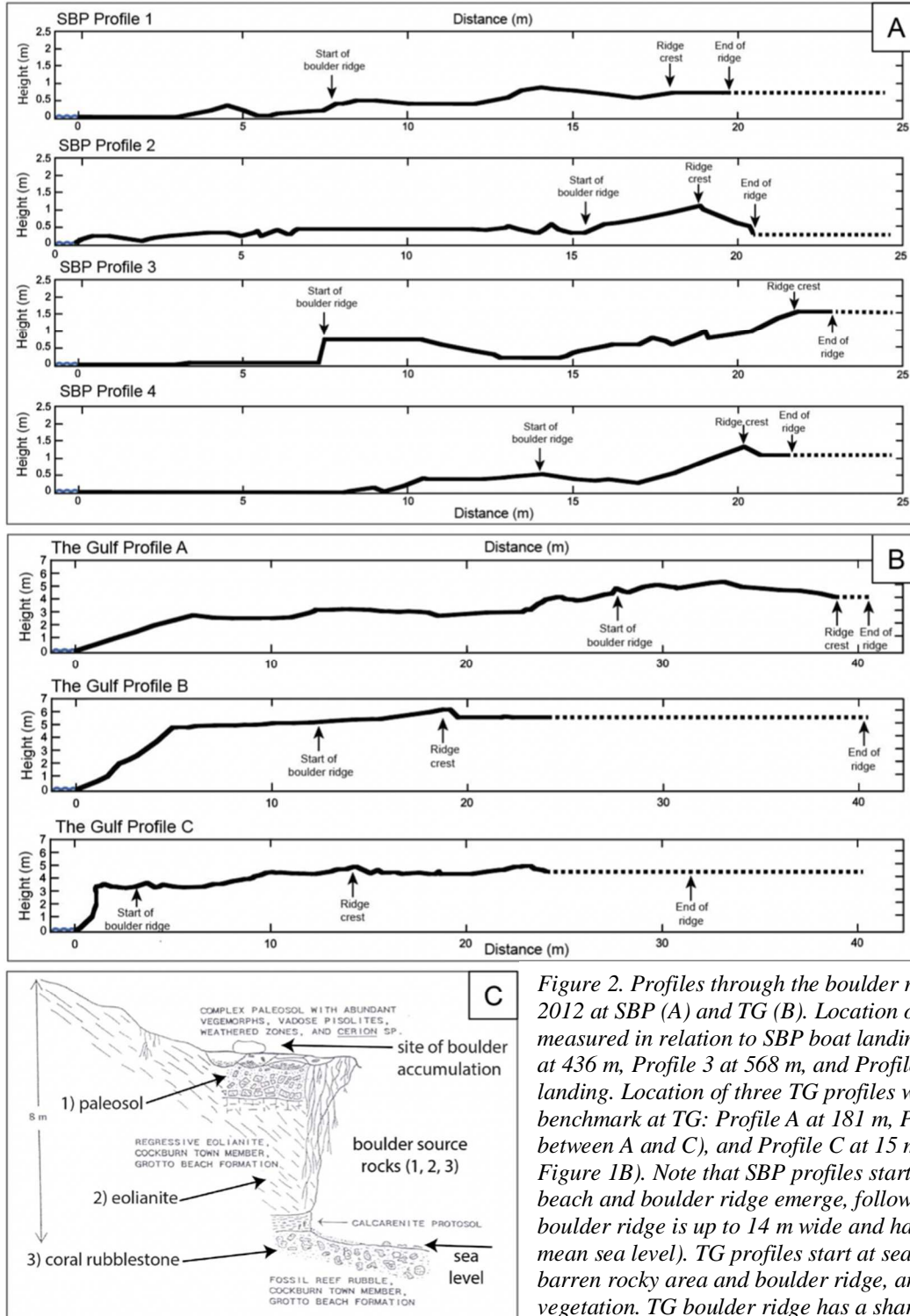

Figure 2. Profiles through the boulder ridges measured in January 2012 at SBP (A) and TG (B). Location of four SBP profiles was measured in relation to SBP boat landing: Profile 1 at 147 m, Profile 2 at 436 m, Profile 3 at 568 m, and Profile 4 at 630 m east of the boat landing. Location of three TG profiles was measured in relation to a benchmark at TG: Profile A at 181 m, Profile B at 98 m (midpoint between A and C), and Profile C at 15 m west of the benchmark (see Figure 1B). Note that SBP profiles start at sea level and then the rocky beach and boulder ridge emerge, followed by maritime forest. SBP boulder ridge is up to 14 m wide and has a low crest (~1.5 m above mean sea level). TG profiles start at sea level, followed by steep cliffs, a barren rocky area and boulder ridge, and end in dense shrub vegetation. TG boulder ridge has a sharp crest, and is on a cliff bench 3-5 m above mean sea level. C) Pleistocene carbonate succession exposed in TG cliffs (from Carew and Mylroie 1985). Note the top of coral reef exposed at modern-day sea level, and the three identified source rocks for boulders deposited by storms on top of TG cliffs.

Table 1. Comparison summary between characteristic features of Singer Bar Point (SBP) vs The Gulf (TG) sites.

Features:	SBP	TG
Boulders	Generally smaller and well rounded	Large, irregular, angular
Boulder ridge	Crest broad, slopes gentle	Crest sharp, well defined
Offshore shelf	Wide, protected	Narrow, open
Wave energy	Gentle, but constant fair-weather waves action	Powerful, even in fair-weather conditions

Table 2. Data on boulders along transects at SBP (A) and TG (B) shown in Figure 2.

A)

Site	Place on Profile (m)	Boulder No.	X Axis (cm)	Y axis (cm)	Z Axis (cm)	Volume (cm³)	Mass (kg)	Probable Comp.	Shape
1	13.4	1	130	138	23	412620	792	Eolianite	Irregular
1	14.6	2	66	73	25	120450	231	Eolianite	Irregular
1	18.1	3	32	37	5	5920	11	Paleosol	Tabular
1	19.1	4	49	29	20	28420	55	Paleosol	Irregular
2	16.0	1	57	36	14	28728	55	Paleosol	Tabular
2	16.3	2	22	32	9	6336	12	Eolianite with Paleosol	Irregular
2	19.9	3	45	30	4	5400	10	Beach Rock	Irregular
3	17.8	1	107	62	15	99510	191	Paleosol	Irregular
3	18.7	2	76	85	5	32300	62	Eolianite with Paleosol	Tabular
3	20.2	3	54	38	6	12312	24	Paleosol	Irregular
3	21.2	4	45	71	6	19170	37	Paleosol	Irregular
3	21.9	5	87	36	10	31320	60	Paleosol	Irregular
4	12.8	1	160	184	16	471040	904	Paleosol	Irregular
4	14.3	2	42	85	22	78540	151	Subtidal	Irregular
4	14.4	3	55	33	14	25410	49	Paleosol	Tabular
4	14.7	4	45	60	12	32400	62	Subtidal	Irregular
4	15.2	5	21	37	7	5439	10	Paleosol	Irregular
4	15.6	6	47	28	4	5264	10	Shelly Calcaranite	Tabular
4	17.2	7	37	27	7	6993	13	Subtidal	Irregular
4	18.6	8	24	30	8	5760	11	Eolianite	Irregular

B)

Site	Place on Profile (m)	Boulder No.	X Axis (cm)	Y axis (cm)	Z Axis (cm)	Volume (cm³)	Mass (kg)	Probable Comp.	Shape
A	23.0	1	32	32	12	12288	24	Paleosol	Irregular
A	24.1	2	85	73	42	260610	500	Paleosol	Irregular
A	25.0	3	57	27	35	53865	103	Coral Rubblestone	Irregular
A	26.8	4	33	38	13	16302	31	Eolianite	Rectangle
A	30.0	5	51	102	40	208080	400	Paleosol	Irregular
A	30.7	6	57	39	10	22230	43	Eolianite	Irregular
B	13.5	1	140	106	17	252280	484	Paleosol	Tabular
B	14.1	2	120	43	15	77400	149	Paleosol	Tabular
B	14.9	3	70	64	15	67200	129	Paleosol	Irregular
B	16.4	4	118	69	17	138414	266	Subtidal	Irregular
B	17.1	5	33	32	9	9504	18	Subtidal	Tabular
B	18.0	6	41	53	12	26076	50	Paleosol	Tabular
B	18.7	7	90	37	21	69930	134	Subtidal	Irregular
C	9.00	1	43	22	17	16082	31	Coral Rubblestone	Tabular
C	9.75	2	21	35	20	14700	28	Paleosol	Irregular
C	10.40	3	150	88	29	382800	735	Paleosol	Irregular
C	11.80	4	62	45	17	47430	91	Paleosol	Irregular
C	12.80	5	52	43	13	29068	56	Coral Rubblestone	Tabular
C	14.20	6	101	92	17	157964	303	Paleosol	Tabular
C	15.75	7	57	47	18	48222	93	Paleosol	Irregular
C	16.30	8	45	44	34	67320	129	Paleosol with Coral Encrusters*	Irregular
C	18.90	9	48	36	8	13824	27	Paleosol (Flipped)	Tabular

Table 3. Data on 15 largest boulders at SBP (A) and 12 largest boulders at TG (B) documented in January 2012.

A)

Boulder No.	X Axis (cm)	Y Axis (cm)	Z Axis (cm)	Volume (cm³)	Mass (kg)
1	130	130	25	422500	811
2	120	70	50	420000	806
3	85	70	15	89250	171
4	200	105	15	315000	605
5	240	120	40	1152000	2212
6	140	100	14	196000	376
7	130	105	14	191100	367
8	170	125	15	318750	612
9	125	120	50	750000	1440
10	190	150	25	712500	1368
11	185	130	20	481000	924
12	310	225	30	2092500	4018
13	205	140	20	574000	1102
14	145	100	20	290000	557
15	205	185	30	1137750	2184

B)

Boulder No.	X Axis (cm)	Y Axis (cm)	Z Axis (cm)	Volume (cm³)	Mass (kg)
1	185	75	65	901875	1732
2	215	110	15	354750	681
3	200	155	25	775000	1488
4	155	125	55	1065625	2046
5	215	130	20	559000	1073
6	205	160	30	984000	1889
7	260	210	20	1092000	2097
8	190	170	25	807500	1550
9	140	120	40	672000	1290
10	210	145	55	1674750	3216
11	215	160	25	860000	1651
12	300	265	30	2385000	4579

All boulders were eroded from the seaward rocky coast, transported and deposited by high-energy storm waves. Clasts of smaller size and better rounding are more common at SBP than TG, indicating multiple events of movement and milling in the surf and/or along the rocky shore prior to deposition along this low-profile coast, as compared to the high cliff-profile TG coast (Figure 2C). The presence of larger boulders and fossil coral rubblestone boulders at TG indicates that much stronger storm waves were

97

required to form and move them in this setting (Dwyer *et al.* 2013).

Impact of Hurricanes Sandy (October 2012) and Joaquin (October 2015)

Similar to Hurricane Irene (August 2011), Hurricane Sandy passed about 80 km (50 miles) to the west of San Salvador Island as a Category 1 to 2 storm on October 25, 2012 (Figure 3A). According to personal communication with Dr. Tom Rothfus (Director of the Gerace Research Centre at that time), minimal island infrastructure damage resulted, and there were no major coastal effects. October 26 was relatively quiet on San Salvador, but on the following day, a strong wave surge began to affect the coast. The largest waves pounded the west and south coasts for 2 days and only diminished on October 29. Considerable coastal erosion resulted, particularly along Fernandez Bay (west coast) and on the south coast between The Gulf and The Cut (our TG study area).

In early February 2013, we resurveyed the largest SBP and TG boulders, which were originally located, measured, and photographed in January 2012 (Table 3). All 15 SBP boulders were easily relocated, indicating that Hurricane Sandy generated only minor coastal effects here. Although a few boulders experienced some movement (e.g., boulder 7 moved inland about 2.5 m; Figure 4), the background of smaller boulders and clasts changed significantly around many of the boulders (Figures 4 and 5). Boulders located to the east of Singer Bar Point did not exhibit position change and showed less background changes than those to the west of the point, confirming local observations that the wave surge effects from Hurricane Sandy were greatest along San Salvador's west and south coasts.
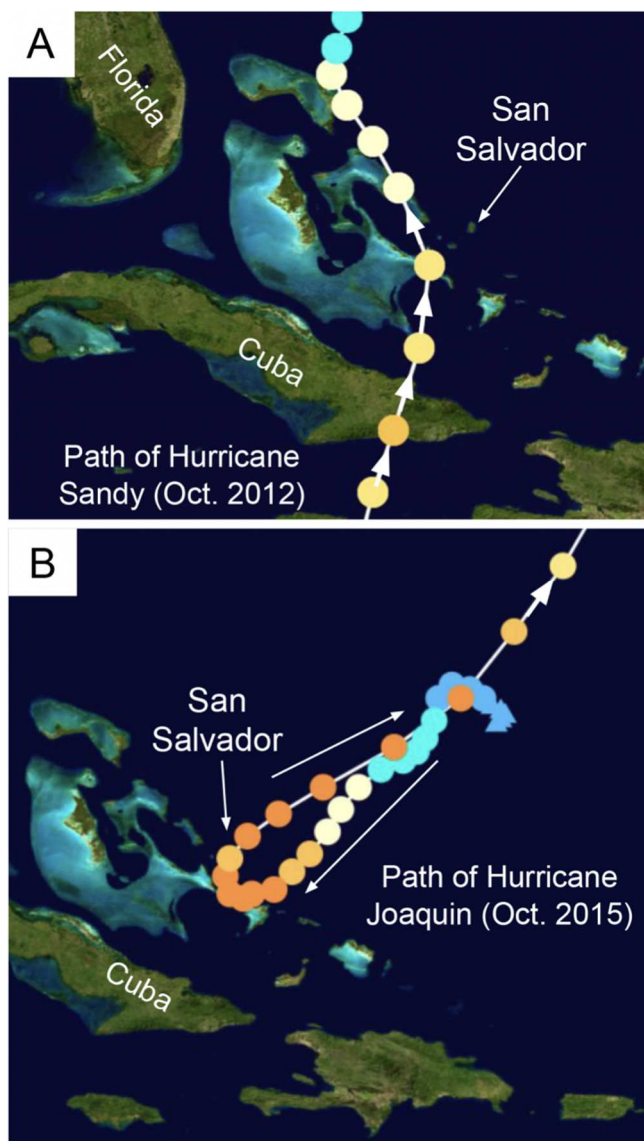

Figure 3. Hurricane pathways. A) Sandy (October 2012) passed about 80 km (50 miles) west of San Salvador and weakened as it moved north from Category 2 (dark yellow circle) to Category 1 (light yellow) and tropical storm (teal circle). B) Joaquin started as a tropical depression (light blue symbols) in the Atlantic to the NE of The Bahamas in late September 2015. It strengthened to Category 4 (dark orange circle) as it moved SW towards The Bahamas, before it made a sharp turn back to the NE and its eye passed directly over San Salvador as a strong Category 3 (light orange circle) hurricane in early October 2015 (source: National Hurricane Center).
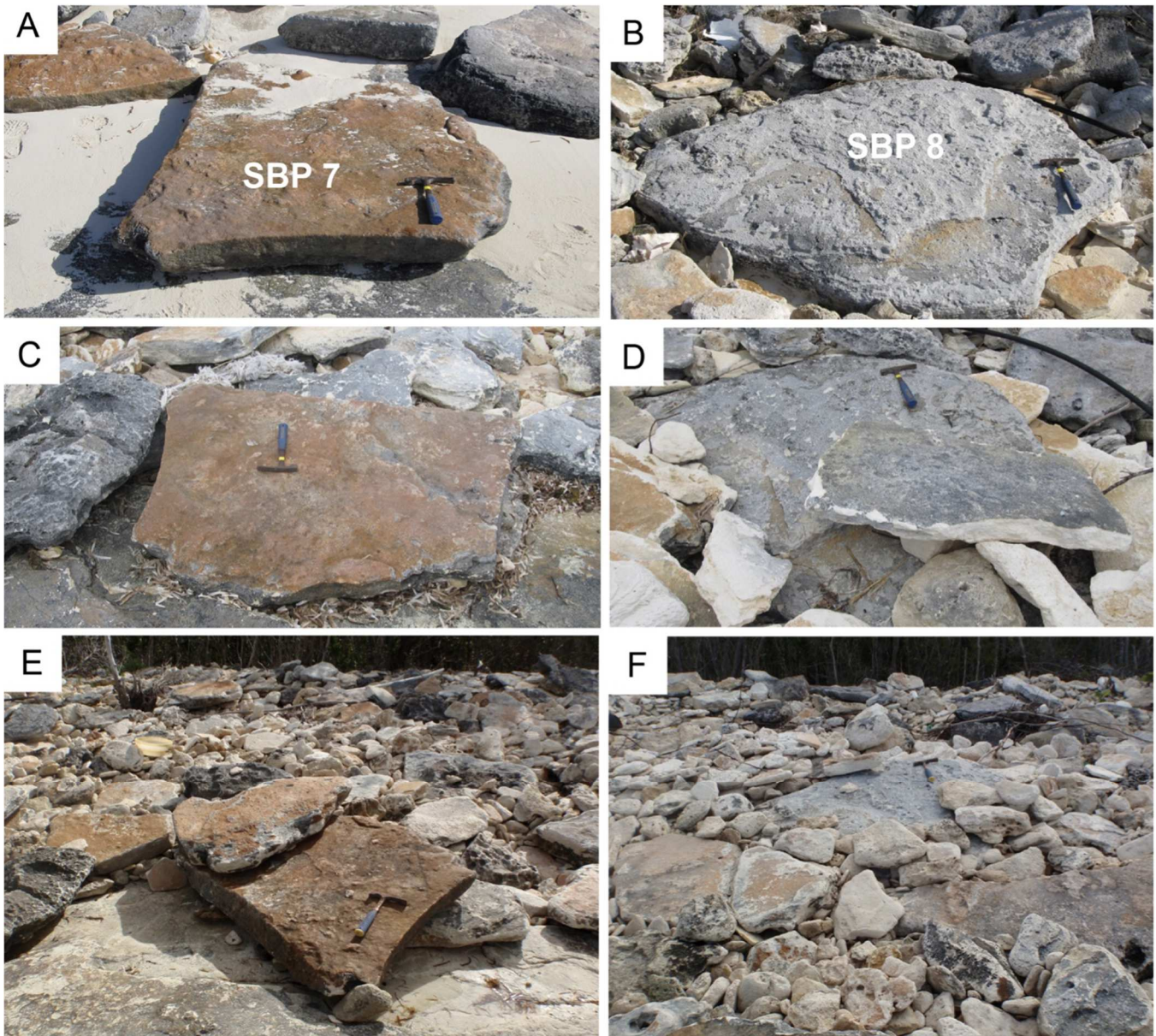
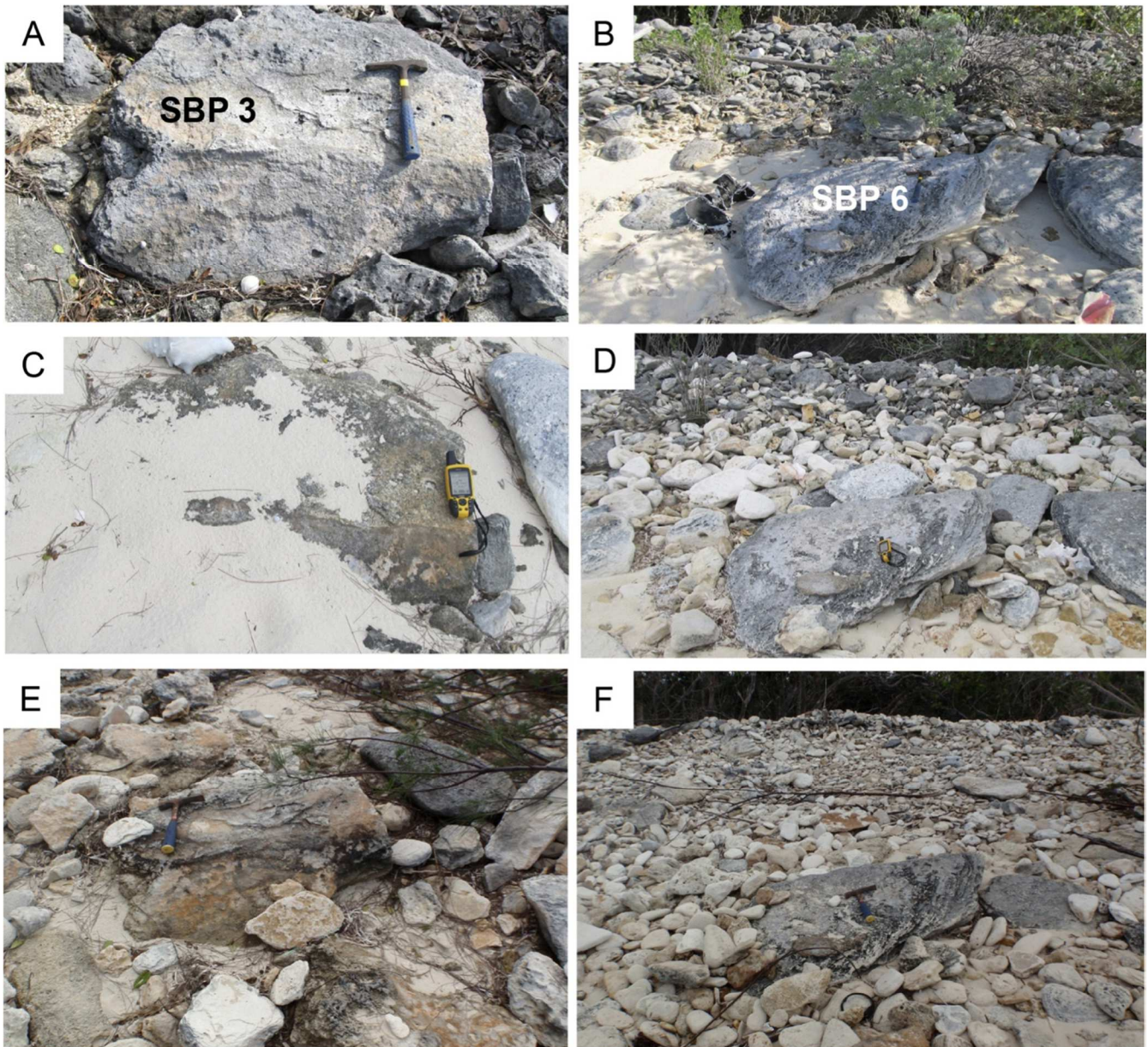*Figure 4. Examples of modifications to boulders at SBP through time. Left column: Boulder 7 (~350 kg); Right column: Boulder 8 (~600 kg). A & B) before Hurricane Sandy (January 2012); C & D) after Hurricane Sandy (February 2013); E & F) after Hurricane Joaquin (January 2016). Hammer for scale and to mark the location of boulders. Boulder 7 was moved about 2.5 m inland (to the south) by Hurricane Sandy (4C), and was transported an additional 3 m to the west and rotated ~180° by Hurricane Joaquin, which also deposited large clasts on top of it and made some new dents in its surface (4E). No major change in the location of boulder 8 was noted since January 2012, but after Sandy and Joaquin this boulder was partially buried in a new arrangement of clasts (4D & F).*

Figure 5. Additional examples of modifications to boulders at SBP through time. Left column: Boulder 3 (~170 kg); Right column: Boulder 6 (~375 kg). A & B) before Hurricane Sandy (January 2012); C & D) after Hurricane Sandy (February 2013); E & F) after Hurricane Joaquin (January 2016). Hammer and GPS unit for scale and to mark the location of boulders. Even though these boulders have not moved since January 2012, the surrounding sediment (sand and smaller clasts) experienced significant changes through time.

This was further supported by our survey of The Gulf area where the effects of Hurricane Sandy were profound (Figures 6 and 7). Two of 12 original boulders (numbers 1 and 3) could not be relocated in the 2013 survey, and there were scour zones at their former locations (Table 4). Other examples of boulder modifications include 90° rotation of boulder 2, and breakage of its upper quarter (the broken segments could not be located). Boulder 4 was moved inland about 3 m, and boulder 5 moved about 9.5 m to the west (Figure 6C). The largest boulder (#12, ~4.5 tons) did not move, but it exhibited the scar of a fresh break on its forward edge. The boulder leaning up against its right side in 2012 was gone, and new clasts surrounded the boulder in the aftermath of Hurricane Sandy (Figure 7D). None of the boulder movement and breakage would have been obvious without knowledge from the pre-storm survey.
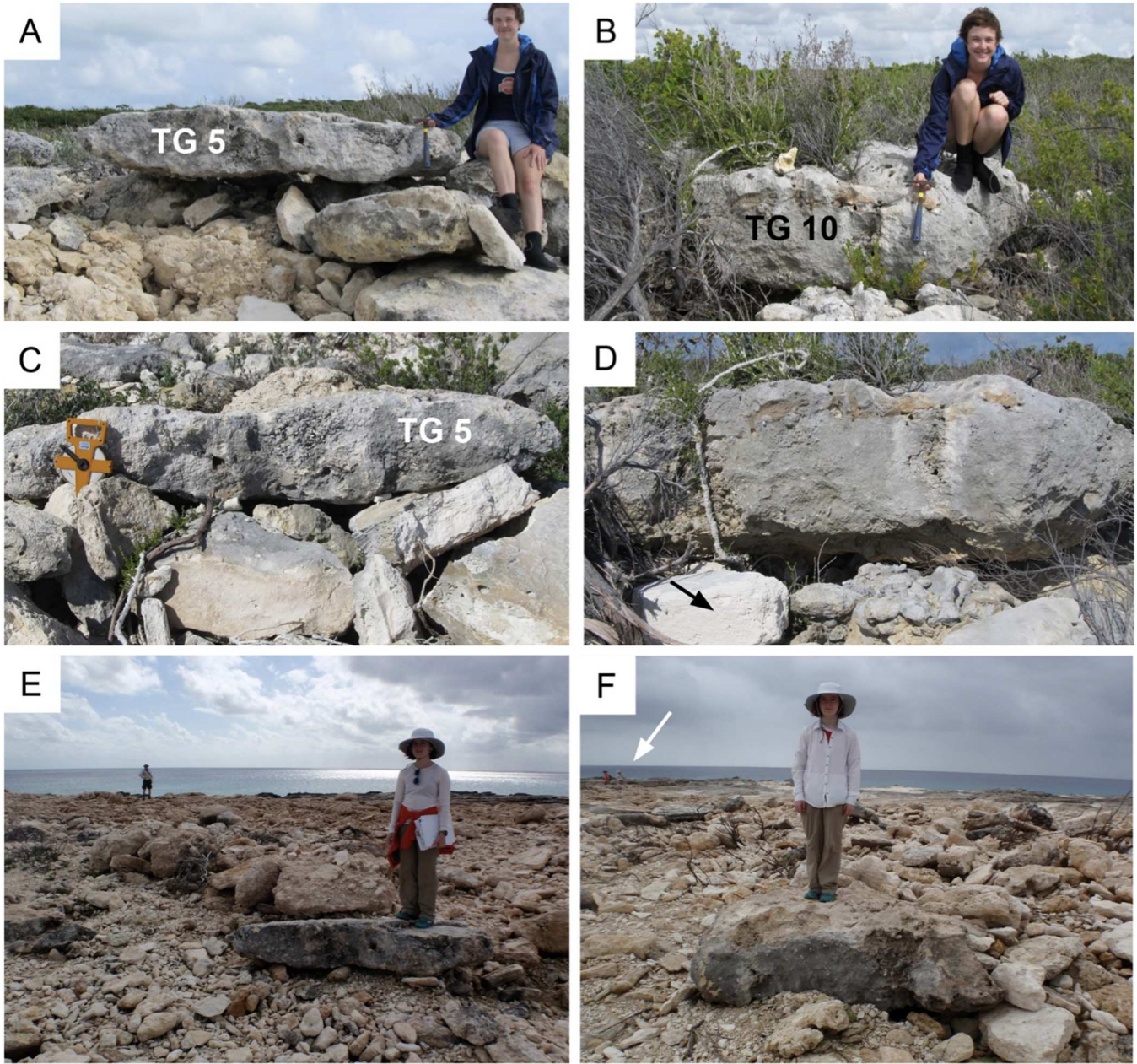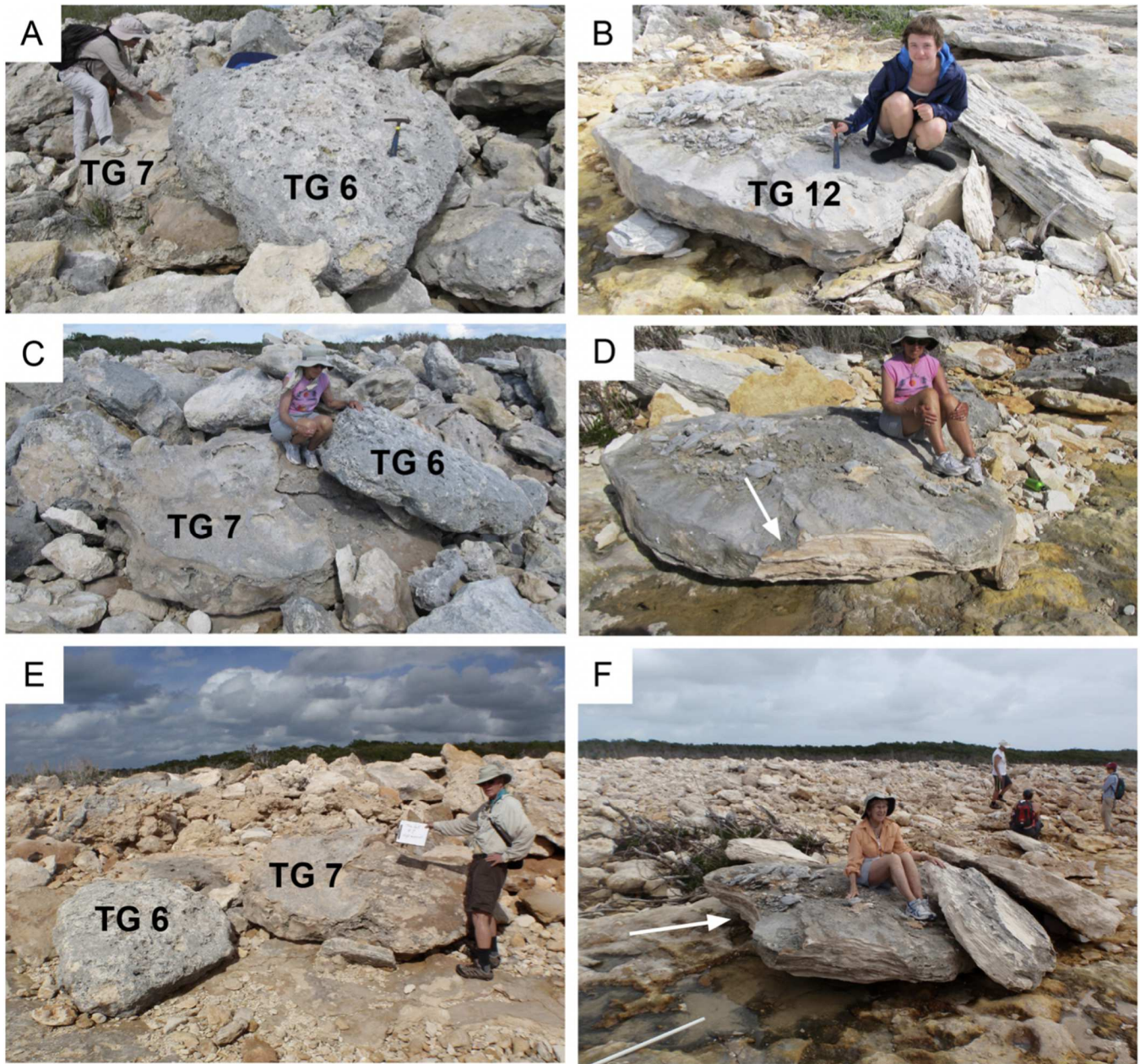
Figure 6. Examples of modifications to boulders at TG through time. Left column: Boulder 5 (~1 ton); Right column: Boulder 10 (~3 tons). A & B) before Hurricane Sandy (January 2012); C & D) after Hurricane Sandy (February 2013); E & F) after Hurricane Joaquin (January 2016). Hurricane Sandy waves moved boulder 5 about 9.5 m to the west (6C), but boulder 10 remained in its original place despite some changes in the surrounding vegetation and deposition of a new large clast (arrow) in front of it (6D). Hurricane Joaquin waves moved boulders 5 and 10 about 20 and 26 m inland to the NNW, respectively (6E and F; person in front is standing on transported boulders and people in distance (arrow in 6F) are at their former location).

Figure 7. Additional examples of modifications to boulders at TG through time. Left column: Boulders 6 and 7 (~2 tons each); Right column: Boulder 12 (~4.5 tons). A & B) before Hurricane Sandy (January 2012); C & D) after Hurricane Sandy (February 2013); E & F) after Hurricane Joaquin (January 2016). Hurricane Sandy did not move these large boulders, but there are noticeable changes in the surrounding sediment, and boulder 12 also lost one corner (arrow in 7D). Hurricane Joaquin waves moved boulder 6 about 4 m W over boulder 7, which maintained about the same location, while smaller surrounding clasts were stripped away (7E). Boulder 12 has not moved since the start of our monitoring, but in Joaquin it lost another edge (arrow) and new smaller boulders were deposited and now lean on it (7F).

Table 4. Status of TG boulders 2012-2016 and calculation of minimum velocity needed to initiate boulder transport.

TG Boulder	Size (m)	*Mass (kg)	Composition	†Status	✦flow velocity (m/s) - sliding	✦flow velocity (m/s) - rolling
1	1.85 x 0.75 x 0.65	1732	coral rubblestone	missing (Sandy)	2.6	3.2
2	2.15 x 1.1 x 0.15	681	eolianite with caliche	missing	2.7	4.3
3	2 x 1.55 x 0.25	1488	eolianite with caliche	missing (Sandy)	3.3	5.4
4	1.55 x 1.25 x 0.55	2046	coral rubblestone	missing	3.2	5.1
5	2.15 x 1.3 x 0.2	1073	coral rubblestone	moved 20 m NNW	3.0	4.9
6	2.05 x 1.6 x 0.3	1889	coral rubblestone	moved 4 m W	3.4	5.7
7	2.6 x 2.1 x 0.2	2097	eolianite with thick paleosol	slight movement/ rotation	3.5	5.2
8	1.9 x 1.7 x 0.25	1550	eolianite with thick paleosol	moved 8 m (?) NNW	3.4	5.5
9	1.4 x 1.2 x 0.4	1290	soil breccia	missing	3.1	5.2
10	2.1 x 1.45 x 0.55	3216	coral rubblestone	moved 26 m NNW	3.4	5.6
11	2.15 x 1.6 x 0.25	1651	eolianite with caliche	missing	3.3	5.4

* calculated using 2.4 g/cm³ for limestone density and by subtracting 20% to account for porosity and irregular size
† October 2012 Hurricane Sandy; all other boulders moved during October 2015 Hurricane Joaquin
✦ calculated using hydrodynamic equations by Nandasena et al. (2011); dependent on boulder size, density of boulders and water, coefficients of lift, drag, gravity, and slope angle (here kept at zero)

Hurricane Joaquin made landfall on islands of the central Bahamas in October 2015, with significant coastal effects (Berg, 2016). The storm was Category 4 at its strongest, but Category 3 with sustained winds of 120-130 mph when its eye passed directly over San Salvador on October 1-3, 2015, impacting the island from multiple directions over several days (Figure 3B). This storm caused major infrastructure damage to about 80% of the buildings, roads, utilities, and the airport on San Salvador (Savarese *et al.* 2016, 2017).

Observations at or study sites in January 2016 revealed only modest modifications at SBP (Glumac *et al.* 2016; Jahan *et al.* 2016). We documented the movement of only one of 15 boulders: boulder 7, ~350 kg in weight, was rotated ~180°, transported about 3 m to the west, had another large clast on top of it, and new dents on its surface (Figure 4E). We also observed changes to the clasts and sediment in the vicinity of the remaining boulders: some were no longer buried in sand, and many had new clasts, as large as 40 cm in diameter, surrounding them (Figures 4 and 5).

In contrast, we documented major changes to TG, where we were unable to relocate 5 of the remaining 10 original boulders (Table 4). At TG, storm waves overtopped the coastal cliffs, causing erosion at the leading edge and extensive landward movement of boulders (Glumac and Curran 2018). New boulders, as large as 3 m in diameter and weighing ~4.5 tons, were generated, and blocks from prior storms, estimated to weigh 1-3 tons, moved up to 26 m inland (Figures 6 and 7; Table 4). Our calculations indicate that minimum wave-generated flow velocities needed to initiate transport of these boulders ranged between 2.6 and 5.7 m/s (Table 4; equations from Nandasena *et al.* 2011). The formerly sharp-crested, narrow boulder ridge was modified into a larger and much broader boulder field, ~6.3 ha in area, stripped of vegetation (Figure 8). The principal coastal road was damaged and inundated by rock debris and sand (Figure 8B). The southern edge of the boulder ridge moved landward by 4-5 m exposing an underlying Pleistocene/Holocene boundary *terra rossa* paleosol (Figure 8D), which stands out in aerial images and marks the extent of storm erosion (Figure 8E). Storm erosion also exhumed an older portion of the boulder ridge, characterized by a variety of clasts partially lithified within an iron-oxide rich matrix.
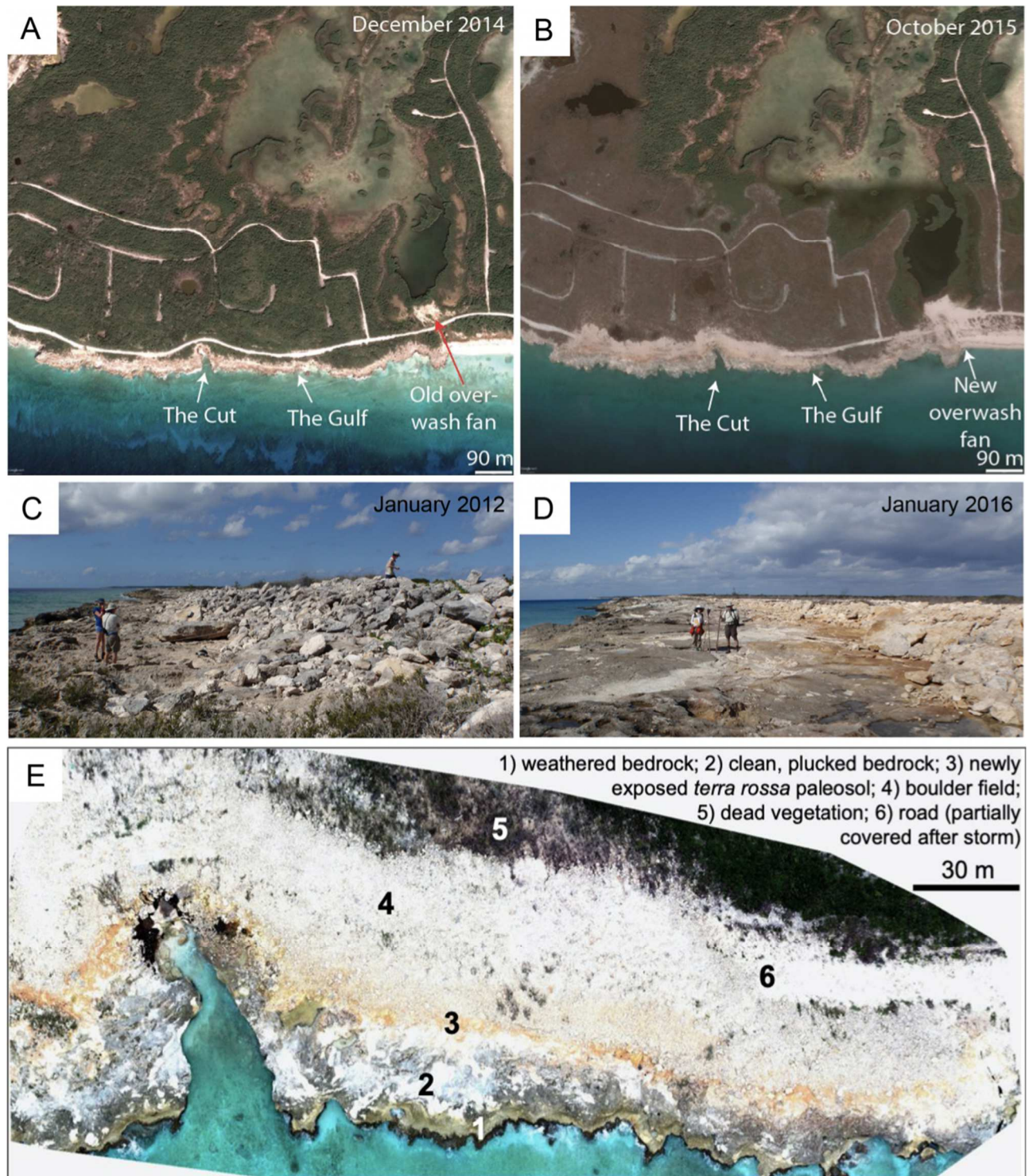
Figure 8. Modifications to the TG area by Hurricane Joaquin. Note: our main study area is between The Cut and The Gulf embayments. A & B) Google Earth images before (December 2014) and after (October 2015) Hurricane Joaquin. Note major vegetation damage (brown areas) generated by Hurricane Joaquin, the coastal road inundated by storm debris, including large boulders, and a new fan deposited by overwash east of The Gulf (8B). C & D) Photographs of the boulder ridge before (January 2012) and after (January 2016) Hurricane Joaquin. The formerly sharp-crested, narrow TG boulder ridge (8C) was modified into a larger, broad boulder field (8D), stripped of vegetation, and partially covering the road (8B). The southern edge of the boulder ridge moved landward by 4-5 m exposing an underlying Pleistocene/Holocene boundary terra rossa paleosol (dark brown areas in 8D), which stands out in aerial images (8E, January 2016) and marks the extent of storm erosion.

Our future research efforts will include study of the origin and lithification of this welded ridge.

Implementation of Drone (2016-Present) and RFID (June 2019-Present) Technologies

Post-hurricane Joaquin, in January 2016, we started to use drones for high-resolution imaging of our study area to document storm impact (Figure 9) and to form a baseline for future comparisons (Perlmutter *et al.* 2016; Glumac and Curran 2017). In January 2017, post-Hurricane Matthew (October 2016), which passed too far west from San Salvador to have any major impact, we added 12 new boulders (boulders 13-24) and additional drone imagery to our monitoring program at the TG site (Figure 9C and D).

Relocation of boulders after major storms by using only their photos, descriptions and former GPS locations proved to be rather difficult and also kept our boulder database relatively small (Figure 9). We addressed these problems by application of RFID technology in June 2019 when >50 boulders were tagged at each study site (Figure 10). Their locations were checked in January 2020, after the 2019 hurricane season, and will continue to be monitored into the future. Since there were no major hurricanes that impacted San Salvador in 2019 (Hurricane Dorian passed too far north to have any impact), we observed no movement of tagged boulders at TG, but our January 2020.
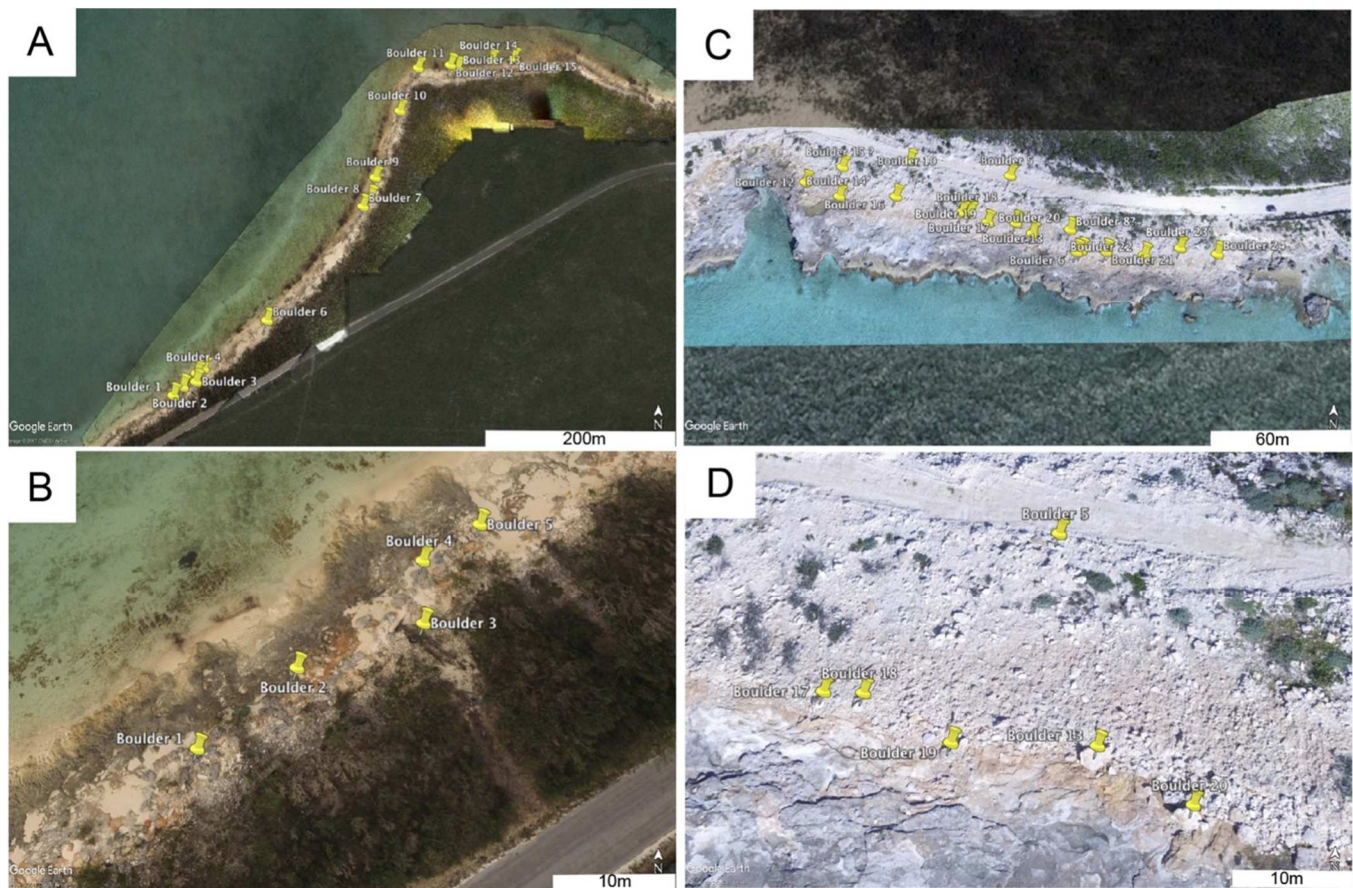

Figure 9. Drone images of SBP (A & B, from January 2016) and TG (C & D, from January 2017, with addition of new boulders). A & C) Entire sites with all boulders (pined) superimposed on Google Earth background to show the difference in resolution between these two sets of images. GPS location of SBP boulders: from N24°07.055' W74°28.640' (Boulder 1) to N24°07.237' W74°28.432' (Boulder 15); TG boulders: from N23°56.813' W74°30.759' (Boulder 1 original location) to N23°56.824' W74°30.805' (Boulder 12); B & D) Close-ups highlighting high-resolution of drone images. Dark brown Pleistocene/Holocene boundary terra rossa paleosol and partially cleared coastal road can be seen in 9D. Scale: A) 200 m; B & D) 10 m; C) 60 m.
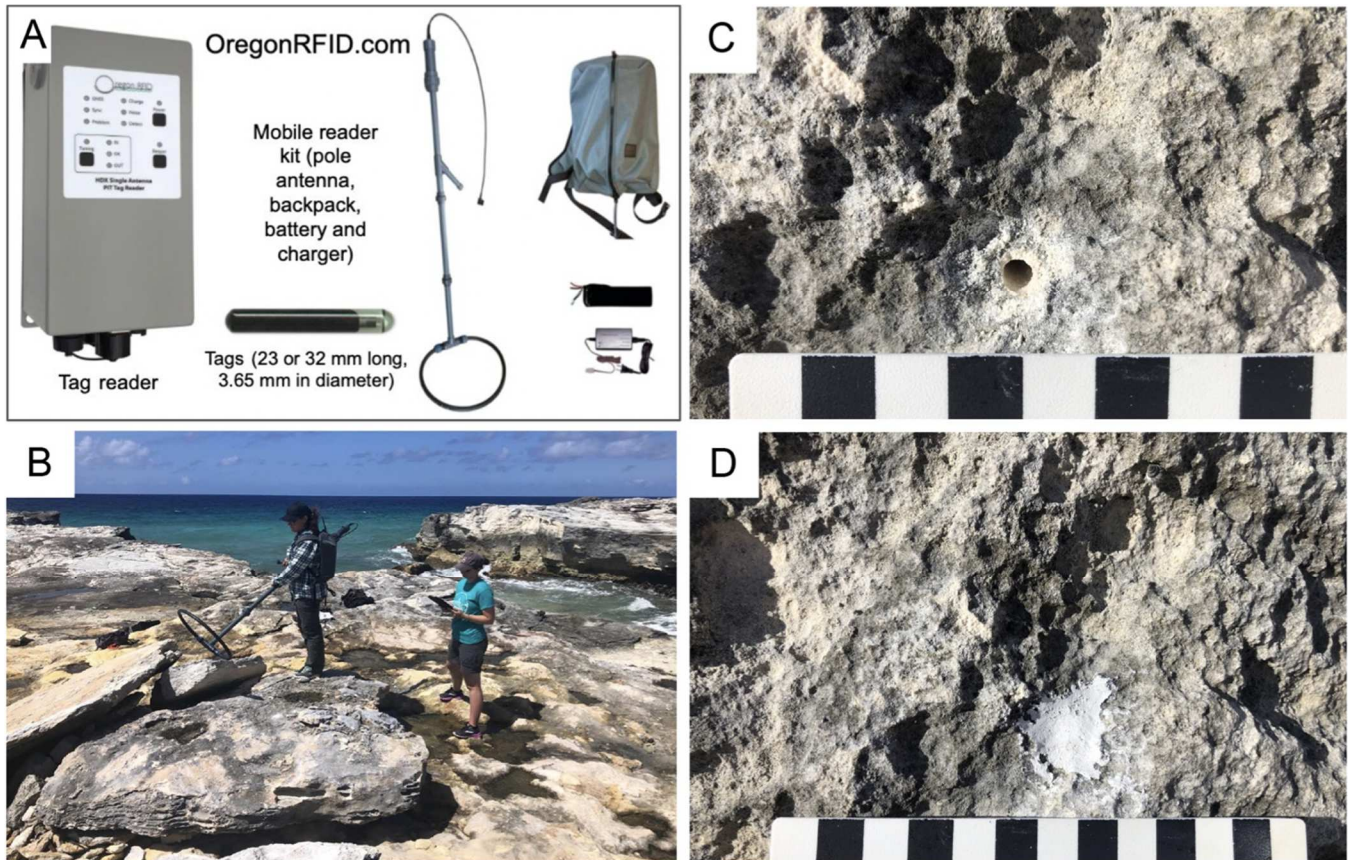
Figure 10. RFID (radio frequency identification) technology. A) System components (from: www.OregonRFID.com). B) Application of RFID at TG. C) Drilled hole for tag inserting. Scale in cms. D) Patched hole with inserted tag. Note its very small size and inconspicuous appearance.

observations documented significant movement of cobbles and smaller boulders by winter storms (i.e. from cold fronts) at SBP

This documentation was possible because RFID technology allowed us to tag and relocate such smaller clasts, thus substantially improving our monitoring efforts. The results of this continuing monitoring will be in the focus of our future presentations and publications.

CONCLUSIONS

1) Our long-term monitoring of storm-deposited boulder ridges along rocky shorelines of San Salvador Island, Bahamas, aims at documenting changes in ridge morphology and distribution, and the direction and amount of movement of individual boulders to gain insights into intensity and effects of storms impacting this small, low relief, tropical carbonate island.

2) Monitoring of storm impact at our two study sites in January 2013, 2016, and 2017, after Hurricanes Sandy (October 2012), Joaquin (October 2015), and Matthew (October 2016), respectively, indicated only modest modifications to Singer Bar Point along the reef- and lagoon-protected gently seaward-sloping northern coast, and major changes to The Gulf on a cliff bench, 3-5 m above mean sea level, along the high-energy southern coast, where we were unable to relocate 2 boulders post-Sandy, and 5 of the remaining 10 original boulders after Joaquin.

3) Even though documentation of boulder movement allows calculation of minimum flow velocity required to initiate their transport, the lack of adequate tagging made it challenging or impossible to relocate many individual boulders after major storms. This problem was addressed by application of RFID (radio frequency identification) tagging in June 2019 when >50 boulders and cobbles were tagged at each study

site using PIT (passive integrated transponder) tags, which are inductively charged by the reader and can remain operational for decades.

4) In conjunction with continuing high-resolution drone imaging, use of tagging that can uniquely identify an object within a large population allows significant increase in our database and improvement of these long-term monitoring efforts.

ACKNOWLEDGMENTS

LITERATURE CITED

Berg, R. (2016). Hurricane Joaquin. National Hurricane Center Tropical Cyclone Report, 36 p.

Carew, J.L., and Mylroie, J.E. (1985). Pleistocene and Holocene stratigraphy of San Salvador Island, Bahamas, with reference to marine and terrestrial lithofacies at French Bay. *In* Curran, H.A., ed., Guidebook for Geological Society of America, Orlando Annual Meeting Field Trip #2, Fort Lauderdale, Florida. CCFL Bahamian Field Station, p. 11-61.

Cox, R., Jahn, K.L., Watkins, O.G., and Cox, P. (2018). Extraordinary boulder transport by storm waves (west of Ireland, winter 2013–2014), and criteria for analysing coastal boulder deposits. Earth-Science Reviews, v. 177, p. 623-636.

Cox, R., Zentner, D.B., Kirchner, B.J., and Cook, M.S. (2012). Boulder ridges on the Aran Islands (Ireland): Recent movements caused by storm waves, not tsunami. The Journal of Geology, v. 120, p. 249-272.

Curran, H.A., Delano, P., White, B., and Barrett, M. (2001). Coastal effects of Hurricane Floyd on San Salvador Island, Bahamas. *In* Greenstein B., and Carney C., eds., Proceedings of the 10ᵗʰ Symposium on the Geology of the Bahamas and Other Carbonate Regions. Gerace Research Center, San Salvador, Bahamas, p. 1-12.

Dwyer, C., Glumac, B., and Curran, H.A. (2013). Storm-deposited boulder ridges on San Salvador Island, Bahamas: characteristics and implications for coastal development. Southeastern Section, Geological Society of America Meeting Abstracts with Programs, v. 45(2), p. 14.

Glumac, B., and Curran, H.A. (2017). Storm-deposited boulder ridges along rocky

shorelines of San Salvador Island, Bahamas: Long-term monitoring and significance. The 2ⁿᵈ Joint Symposium on the Natural History and Geology of the Bahamas. Gerace Research Centre, San Salvador, Bahamas, p. 7-8.

Glumac, B., and Curran, H.A. (2018). Documenting the generation and transport of large rock boulders by storm waves along the high-energy southern coast of San Salvador Island, Bahamas. American Geophysical Union Annual Fall Meeting, Washington, D.C., Abstract #EP23C-2296.

Glumac, B., Jahan, N. and Curran, H.A. (2016). Monitoring changes in boulder ridges along rocky shorelines of San Salvador Island, Bahamas, as indicators of storm activity. Geological Society of America Abstracts with Programs, Annual Meeting, Denver, Colorado, v. 48(7). doi: 10.1130/abs/2016AM-282135

Hearty, P.J. (1997). Boulder deposits from large waves during the last interglaciation on North Eleuthera, Bahamas. Quaternary Research, v. 48, p. 326-338.

Hearty, P.J., and Tormey, B.R. (2017). Sea-level change and superstorms; geologic evidence from the last interglacial (MIS 5e) in the Bahamas and Bermuda offers ominous prospects for a warming Earth. Marine Geology, v. 390, p. 347–365.

Jahan, N., Glumac, B., and Curran, H.A. (2016). Storm-deposited coastal boulder ridges on San Salvador Island, Bahamas in the aftermath of Hurricane Joaquin. Geological Society of America Abstracts with Programs, Annual Meeting, Denver, Colorado, v. 48(7). doi: 10.1130/abs/2016AM-282132

Kelletat, D., Scheffers, A., and Scheffers, S. (2004). Holocene tsunami deposits on the Bahaman Islands of Long Island and Eleuthera. Zeitschrift für Geomorphologie, v. 48, p. 519-540.

Kindler, P., Mylroie, J.E., Curran, H.A., Carew, J.L., Gamble, D.W., Rothfus, T.A., Savarese, M., and Sealey, N.E. (2010). Geology of Central Eleuthera, Bahamas: A Field Trip Guide for The 15ᵗʰ Symposium on the Geology of the Bahamas and Other Carbonate Regions. Gerace Research Centre, San Salvador, Bahamas, 75 p.

Mylroie, J.E. (2008). Late Quaternary sea-level position: evidence from Bahamian carbonate deposition and dissolution cycles. Quaternary International, v. 183, p. 61-75.

Mylroie, J.E. (2018). Superstorms: Comments on Bahamian fenestrae and boulder evidence from the Last Interglacial. Journal of Coastal Research, v. 34, p. 1471–1483.

Niemi, T.M. (2017). Large boulders on Green Cay, San Salvador Island, The Bahamas. *In* Landry, C.L., and Kjar, D.S., eds., Proceedings of the 1ˢᵗ Joint Symposium on the Natural History and Geology of The Bahamas, June 2015. Gerace Research Center, San Salvador, Bahamas, p. 121-129.

Niemi, T.M., Thomason, J.C., McCabe, J.M., and Daehne, A. (2008). Impact of the September 2, 2004 Hurricane Frances on the coastal environment of San Salvador Island, the Bahamas. *In* Park, L.E., and Freile, D., eds., Proceedings of the 13ᵗʰ Symposium on the Geology of the Bahamas and Other Carbonate Regions. Gerace Research Center, San Salvador, Bahamas, p. 43-64.

Panuska, B.C., Boardman, M.R., Carew, J.L., Mylroie, J.E., Sealey, N.E., and Voegeli, V. (2002). Eleuthera Island Field Trip Guide for The 11ᵗʰ Symposium on the Geology of the Bahamas and Other

Carbonate Regions. Gerace Research Center, San Salvador, Bahamas, 20 p.

Perlmutter, E., Caris, J., Widstrand, A., Curran, H.A., and Glumac, B. (2016). Drone use in rapid assessment of Hurricane Joaquin coastal impact on San Salvador Island, Bahamas. Geological Society of America Abstracts with Programs, Annual Meeting, Denver, Colorado, v. 48(7). doi: 10.1130/abs/2016AM-282290

Rovere, A., Casella, E., Harris, D.L., Lorscheid, T., Nandasena, N.A.K., Dyer, B., Sandstrom, M.R., Stocchi, P., D'Andrea, W.J., and Raymo, M.E. (2017). Giant boulders and Last Interglacial storm intensity in the North Atlantic. Proceedings of the National Academy of Sciences of the United States of America, v. 114, p. 12144-12149.

Rovere, A., Casella, E., Harris, D.L., Lorscheid, T., Nandasena, N.A.K., Dyer, B., Sandstrom, M.R., Stocchi, P., D'Andrea, W.J., and Raymo, M.E. (2018). Reply to Hearty and Tormey: Use the scientific method to test geologic hypotheses, because rocks do not whisper. Proceedings of the National Academy of Sciences of the United States of America, v. 115, E2904–E2905.

Savarese, M., Buynevich, I.V., Caris, J., Curran, H.A., Glumac, B., Park Boush, L., and Kopcznski, K. (2016). Heterogeneous vulnerability to Hurricane Joaquin's influence along the perimeter of San Salvador Island, Bahamas. Geological Society of America Abstracts with Programs, Annual Meeting, Denver, Colorado, v. 48(7). doi: 10.1130/abs/2016AM-282743

Savarese, M., Buynevich, I., Caris, J., Curran, H.A., Glumac, B., Park Boush, L., and Kopcznski, K. (2017). A vulnerability analysis of Hurricane Joaquin's effects along the perimeter of San Salvador Island, Bahamas. Abstracts and Program, The 2nd Joint Conference on the Natural History and Geology of the Bahamas, Gerace Research Centre, San Salvador, Bahamas.

Nandasena, N.A.K., Paris, R., and Tanaka, N. (2011). Reassessment of hydrodynamic equations: Minimum flow velocity to initiate boulder transport by high energy events (storms, tsunamis). Marine Geology, v. 281, p. 70-84.

Walker, S.E., Holland, S.M., and Gardiner, L. (2001). Cockburn Town Fossil Reef: A summary of effects from Hurricane Floyd. *In* Greenstein, B., and Carney, C., eds., Proceedings of the 10th Symposium on the Geology of the Bahamas and Other Carbonate Regions. Gerace Research Center, San Salvador, Bahamas, p. 13-19. .